Journal of Southeast University (English Edition) Vol. 30, No. 4, pp. 489 - 494 Dec. 2014 ISSN 1003—7985

Numerical simulation of typhoon-induced storm surge on the coast of Jiangsu Province, China, based on coupled hydrodynamic and wave models

Xu Sudong[1] Yin Kai[1] Huang Wenrui[2,3] Zheng Wei[1]

([1]School of Transportation, Southeast University, Nanjing 210096, China)
([2]College of Civil Engineering, Tongji University, Shanghai 200092, China)
([3]Department of Civil and Environmental Engineering, Florida State University, Tallahassee, FL 32310, USA)

Abstract: In order to facilitate engineering design and coastal flooding protection, the potential storm surge induced by a typhoon is studied. Using an unstructured mesh, a coupled model which combines the advanced circulation (ADCIRC) hydrodynamic model and simulating waves nearshore (SWAN) model is applied to analyze the storm surge and waves on the coast of Jiangsu Province. The verifications of wind velocity, tidal levels and wave height show that this coupling model performs well to reflect the characteristics of the water levels and waves in the studied region. Results show that the effect of radiation stress on storm surge is significant, especially in shallow areas such as the coast of Jiangsu Province and the Yangtze estuary. By running the coupled model, the simulated potential flooding results can be employed in coastal engineering applications in the Jiangsu coastal area, such as storm surge warnings and extreme water level predictions.

Key words: coast of Jiangsu Province; typhoon storm surge; advanced circulation (ADCIRC) hydrodynamic model; simulating waves nearshore (SWAN) model

doi: 10.3969/j.issn.1003-7985.2014.04.015

Storm surges are a serious natural hazard caused by tropical storm, which can raise the water level of inshore and coastal low-lying areas dramatically and result in coastal flooding. The water levels induced by typhoon storm surges often potentially cause significant loss of life and property. For example, one of the greatest recorded hurricanes in the United States was Hurricane Katrina, which produced the highest recorded storm surge (8.5 m) in recent history[1], and killed 1 833 people through widespread inundation[2]. In China, landfalling tropical typhoons caused direct economic losses of 28.7 billion Yuan and the toll was 472 people each year during the period 1983—2006, accounting for 0.38% of the annual total GDP[3]. Therefore, the potential storm surge induced by typhoon storm surges needs to be studied for engineering design and coastal flooding protection.

There are two major approaches in predicting storm surges[4]. The first one is statistical prediction, which may be fast and simple, however this method is based on the statistics of past events, which makes it difficult to take future specifics into account. The second approach is hurricane storm surge simulation, which has been a powerful tool for predicting storm surges, designing protection systems, evaluating risk, and planning emergency evacuation[5]. Among many hydrodynamic models for storm surge simulations, ADCIRC is one of the widely used models applied to predict storm surges during typhoons[6].

Recently, coupling of hydrodynamic and wave models has been developed in order to increase the accuracy of simulations. Funakoshi et al.[7] demonstrated a practical application of coupling a hydrodynamic model and a wave model for the calculation of storm tide elevations in the St. Johns River (Northeastern Florida), where two coupling procedures were considered, and the model results showed that wind-induced waves can lead to additional water level rises. Dietrich et al.[8] integrated a tightly-coupled ADCIRC + SWAN model, where the ADCIRC and SWAN shared the same mesh and parallel computing infrastructure, a hurricane storm surge simulated by this coupled model displayed high levels of accuracy and efficiency. Sebastian et al.[5] used the ADCIRC + SWAN model to assess the connection between the wind speed and landfall location of Hurricane Ike and storm surges at locations in and around Galveston Bay, and they concluded that the wind speeds increasing by 15% results in an approximately 23% (±3%) higher surge. Xu et al.[9] also successfully applied the ADCIRC and SWAN model to estimate extreme high water levels in different return periods in Colombo, Sri Lanka.

Although the previous research has demonstrated the

Received 2014-07-17.

Biography: Xu Sudong (1980—), male, doctor, associate professor, sudongxu@seu.edu.cn.

Foundation items: The National Natural Science Foundation of China (No. 51209040, 51279134), the Natural Science Foundation of Jiangsu Province (No. BK2012341), the Fundamental Research Funds for the Central Universities (No. SJLX_0087), the Research Fund of Nanjing Hydraulic Research Institute (No. Y213012).

Citation: . Xu Sudong, Yin Kai, Huang Wenrui, et al. Numerical simulation of typhoon-induced storm surge on the coast of Jiangsu Province, China, based on coupled hydrodynamic and wave models[J]. Journal of Southeast University (English Edition), 2014, 30(4): 489 - 494. [doi: 10.3969/j.issn.1003-7985.2014.04.015]

successful application of the ADCIRC + SWAN model in studying the effects of hurricanes in United States, it is necessary to apply the ADCIRC + SWAN model to study storm surges and waves on the coast of Jiangsu Province. In this paper, the ADCIRC + SWAN model is employed to simulate the potential surge setups generated by a typical typhoon and to analyze the effect of radiation stress on storm surges at different depths.

1 Study Area

Jiangsu Province is one of the most prosperous provinces of the People's Republic of China and is located on the coast of the East China Sea. With the rapid economic development of Jiangsu Province, the potential danger from storm surges and high waves, disaster prevention and mitigation have been important concerns. The landfalling tropical typhoons caused direct economic losses of 0.74 billion Yuan and killed 7.4 people each year in Jiangsu Province during the period 1983—2006[3]. Therefore, the underestimation of the storm surge water levels and waves in coastal planning and development may cause disastrous consequences.

On July 28, 2011, Typhoon Muifa (1109) formed into a tropical storm above the northwestern Pacific Ocean. It became a super typhoon twice during its movement toward Chinese mainland. Although Muifa bypassed Shanghai and moved further north instead of striking Jiangsu Province directly, it indeed wreaked havoc in the areas of Liaoning, Shanghai, and Zhejiang. According to Chinese weather websites[10], more than 3.6 million people suffered under the super typhoon, at least 600 houses collapsed and 4 800 houses were damaged, and the direct economic loss was 3.128 billion Yuan. Due to the menacing typhoon, a major sea bridge was closed in Shanghai. Part of the breakwater of a chemical plant located in Dalian collapsed. The typhoon information was provided by the NOAA website. The details of the historical typhoons including hourly typhoon tracking, central pressure as well as the maximum wind speed can be obtained from the NOAA website.

Since the observed datasets of wind speeds, water levels and wave heights during Typhoon 1109 are available for model verification and further study in this paper, Typhoon 1109 is selected to analyze the effects of radiation stress on storm surges.

2 Numerical Model Description

2.1 ADCIRC model

The water surface elevations and vertically averaged velocities are computed by the fully nonlinear two-dimensional, depth-integrated option of the ADCIRC model[11]. The ADCIRC model has been widely used in coastal hydrodynamic modeling and has had many successful applications in coastal numerical modeling[6]. The governing equations are described in space using the linear finite element method and in time using the finite difference method. The basic governing continuity Eq. (1) and momentum Eqs. (2) to (3) of the model are expressed in Cartesian coordinates:

$$\frac{\partial \zeta}{\partial t}+\frac{\partial UH}{\partial x}+\frac{\partial VH}{\partial y}=0 \tag{1}$$

$$\frac{\partial U}{\partial t}+U\frac{\partial U}{\partial x}+V\frac{\partial U}{\partial y}-fV=-\frac{\partial}{\partial x}\left[\frac{p_s}{\rho_0}+g(\zeta-\alpha\eta)\right]+\frac{1}{H}M_X+\frac{\tau_{SX}}{\rho_0 H}-\tau_* U \tag{2}$$

$$\frac{\partial V}{\partial t}+U\frac{\partial V}{\partial x}+V\frac{\partial V}{\partial y}+fU=-\frac{\partial}{\partial y}\left[\frac{p_s}{\rho_0}+g(\zeta-\alpha\eta)\right]+\frac{1}{H}M_Y+\frac{\tau_{SY}}{\rho_0 H}-\tau_* V \tag{3}$$

where t is the time; x, y are the horizontal coordinates, aligned in the East and North directions, respectively; ζ is the free surface elevation; U is the depth-averaged horizontal velocity in x direction; V is the depth-averaged horizontal velocity in y direction; H is the total water column depth, $h+\zeta$; h is the bathymetric depth; $f=2\Omega\sin\varphi$ is the Coriolis parameter; Ω is the angular speed of the earth; φ is the degrees latitude; p_s is the atmospheric pressure at the free surface; g is the acceleration due to gravity; η is the Newtonian equilibrium tide potential; a is the earth elasticity factor; ρ_0 is the reference density of water; τ_{SX} is the applied free surface stress in x direction; τ_{SY} is the applied free surface stress in y direction; $\tau_*=C_f\sqrt{U^2+V^2}/H$ is the bottom stress; C_f is the bottom friction coefficient; $M_X=E_{h2}[\partial^2 UH/\partial x^2+\partial^2 UH/\partial y^2]$ is the depth-integrated momentum dispersion in x direction; $M_Y=E_{h2}[\partial^2 VH/\partial x^2+\partial^2 VH/\partial y^2]$ is the depth-integrated momentum dispersion in y direction; E_{h2} is the horizontal eddy viscosity.

2.2 SWAN model

The SWAN wave model developed by TU Delft was applied for the simulation of storm-induced wind-waves. The governing equation is expressed as[8]

$$\frac{\partial N}{\partial t}+\nabla_{\boldsymbol{x}}\cdot[(\boldsymbol{c}_g+\boldsymbol{U})N]+\frac{\partial c_\sigma N}{\partial \sigma}+\frac{\partial c_\theta N}{\partial \theta}=\frac{S_{tot}}{\sigma} \tag{4}$$

The terms from left to right stand for the change of wave action over time; the propagation of wave action in $\boldsymbol{x}$ space (with the gradient operator $\nabla_{\boldsymbol{x}}$ in geographic space, the wave group velocity $\boldsymbol{c}_g$ and the ambient current vector $\boldsymbol{U}$); depth- and current-induced refraction and approximate diffraction (with propagation velocity or turning rate c_θ); and the shifting of σ due to variations in mean current and depth (with propagation velocity or shifting rate c_σ). The source term S_{tot} represents wave

growth by the following factors: 1) Wind; 2) Action lost due to whitecap, surf breaking and bottom friction; and 3) Action exchanged between spectral components in deep and shallow water due to nonlinear effects.

2.3 Typhoon model

As the main important input boundary conditions of storm surges and wave models, wind and atmospheric pressure are the main factors in creating the storm surge and waves[12]. The accuracy of the input wind field during a typhoon is crucial for the results of modeling storm surge and wave characteristics.

The wind and pressure field for each node of the whole studied area is very important for the hydrodynamic model and can be calculated by wind and pressure formulae, such as the Fujita-Takahashi formula, the Myers formula, the Fujita formula, the McNair's formula, and the Bier Ke formula and so on. According to previous studies in the Pacific region, the Fujita-Takahashi formula has had many successful applications and is the optimal model. In this study, the nested model of the Fujita formula and Takahashi formula is chosen as the typhoon numerical model to calculate its air pressure and wind field. Their distribution form can be expressed as follows:

$$P(r) = P_\infty - \frac{P_\infty - P_0}{\sqrt{1 + 2(r/R)^2}} \qquad 0 \leqslant r \leqslant 2R \tag{5}$$

$$P(r) = P_\infty - \frac{P_\infty - P_0}{1 + r/R} \qquad 2R \leqslant r \leqslant \infty \tag{6}$$

where $P(r)$ is the pressure at a radial distance r from the cyclone center; P_∞ is the ambient or environmental pressure; P_0 is the cyclone central pressure; r is the radius (distance from cyclone center); R is the radius to the point of the maximum wind speed.

When $0 \leqslant r \leqslant 2R$,

$$W_x = C_1 V_x \exp\left(-\frac{\pi}{4}\frac{|r-R|}{R}\right) - C_2\left\{-\frac{f}{2} + \sqrt{\frac{f^2}{4} + \frac{2\Delta P}{\rho_a R^2}\left[1 + 2\left(\frac{r}{R}\right)^2\right]^{-3/2}}\right\} \cdot [(x - x_0)\sin\theta + (y - y_0)\cos\theta] \tag{7}$$

$$W_y = C_1 V_y \exp\left(-\frac{\pi}{4}\frac{|r-R|}{R}\right) + C_2\left\{-\frac{f}{2} + \sqrt{\frac{f^2}{4} + \frac{2\Delta P}{\rho_a R^2}\left[1 + 2\left(\frac{r}{R}\right)^2\right]^{-3/2}}\right\} \cdot [(x - x_0)\cos\theta - (y - y_0)\sin\theta] \tag{8}$$

When $2R \leqslant r \leqslant \infty$,

$$W_x = C_1 V_x \exp\left(-\frac{\pi}{4}\frac{|r-R|}{R}\right) - C_2\left\{-\frac{f}{2} + \sqrt{\frac{f^2}{4} + \frac{\Delta p}{\rho_a R r}\left[1 + \frac{r}{R}\right]^{-2}}\right\} \cdot [(x - x_0)\sin\theta + (y - y_0)\cos\theta] \tag{9}$$

$$W_y = C_1 V_y \exp\left(-\frac{\pi}{4}\frac{|r-R|}{R}\right) - C_2\left\{-\frac{f}{2} + \sqrt{\frac{f^2}{4} + \frac{\Delta p}{\rho_a R r}\left[1 + \frac{r}{R}\right]^{-2}}\right\} \cdot [(x - x_0)\cos\theta - (y - y_0)\sin\theta] \tag{10}$$

where $\Delta p = p_\infty - p_0$, p_∞ is the atmospheric pressure at a remote point from the typhoon center and p_0 is the typhoon central pressure; r is the distance of the station to the central of the typhoon; R is the typhoon parameter; C_1 and C_2 are empirical constants, which are 1.0 and 0.8, respectively; θ is the inflow angle, $\theta = 20°$; ρ_a is the air density; f is the Coriolis force parameter; V_x and V_y are the typhoon forward velocities in x, y direction, respectively.

For the calculation of the wind field, the maximum wind speed of radius R is also a key factor. The following empirical formula has been selected for this study:

$$R = 28.52\tanh[0.087\,3(\varphi - 28)] + 0.2V_c + \frac{12.22}{\exp[(1\,013.2 - p_0)/33.86]} + 37.22 \tag{11}$$

where φ is the typhoon center latitude, (°); p_0 is the typhoon central pressure, hPa; V_c is the speed of the typhoon center, m/s.

3 Model Setup and Verification

3.1 Model setup

The model domain is shown in Fig. 1, which covers not only the major part of East China Sea but also the whole Bohai Sea and the Yellow Sea. There are two open sea boundaries, on the east side at 128° E and on the south side at 25°N. The landwards boundary of the Yangtze estuary is at Jiangyin. The same unstructured finite-element mesh and bathymetry of this studied domain are developed for both storm surge and wave simulation (see Fig. 2). The grid resolution varies from about 50 km on

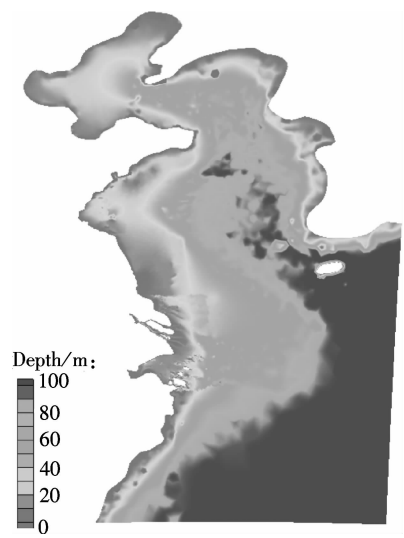

Fig. 1 Model domain and its bathymetry

the edges of the model to about 300 m in the Yangtze estuary near the studied area as shown in Fig. 3. The total number of computational nodes and triangular elements are 31 402 and 59 590.

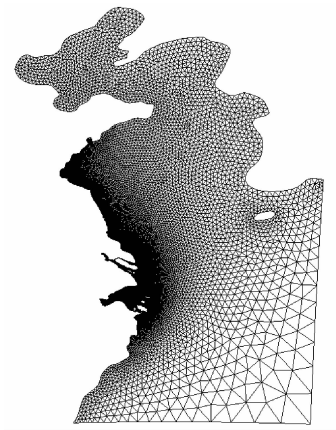

Fig. 2 The model mesh of the studied domain

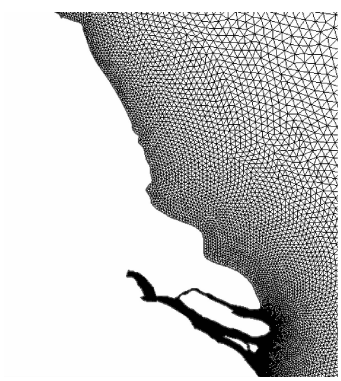

Fig. 3 The model mesh near Jiangsu province

At the open sea boundary, water level conditions induced by astronomical tide have been adopted. The river banks and coastlines are considered as no-flow boundaries and zero-flux constraint boundaries. The ADCIRC model is discretized using a 1 s time step, and the time step for the SWAN model is 5 min. In order to realize the coupling procedure and investigate the effects of wave contributions on the overall storm tide water levels, SWAN provides updated wave field information (gradients of wave radiation stresses) to ADCIRC every 1 h and the ADCIRC model gives feedback concerning water levels and currents to SWAN every 1 h.

3.2 Model verification

To assess its modeling accuracy, the numerical model system was initially applied to reproduce the wind field, storm surge and waves. The stations for model verification are shown in Fig. 4.

The typhoon wind speed model is verified by comparing the observed wind velocity and model simulation during Typhoon 1109. As shown in Fig. 5, model simulation result matches well with the observed dataset. The wind field and pressure field generated by the typhoon model

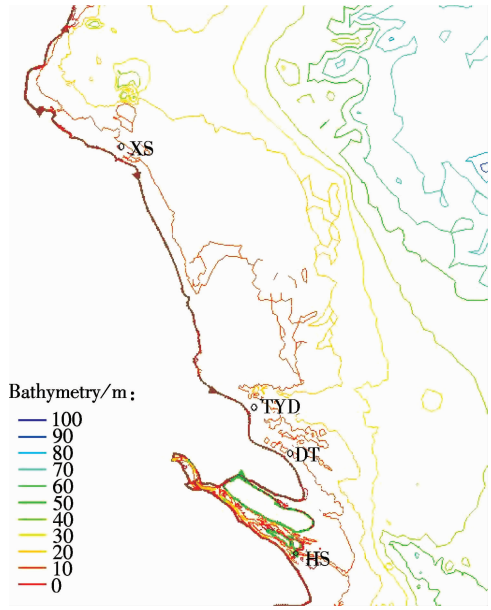

Fig. 4 Stations used for verification (DT—Datang; TYD—Taiyangdao; HS—Hengsha; XS—Xiangshui)

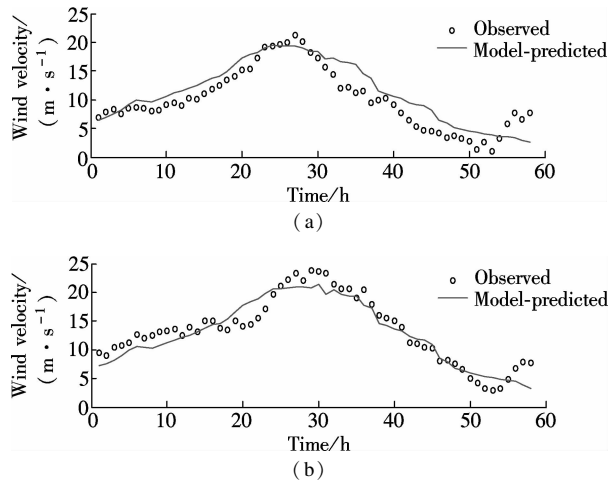

Fig. 5 Comparison between model-predicted and observed wind velocity. (a) Datang station; (b) Taiyangdao station

are used as the forcing factor of the storm surge model and the wave model.

Due to the lack of observed tidal level in the studied domain during Typhoon 1109, a time period from the tidal level hydrograph in 1997 is chosen for hydrodynamic model verification. The comparison shows that the model-predicted tidal level hydrograph is basically consistent with the observed dataset (see Fig. 6).

The wave height during Typhoon 1109 is also verified. Due to the underestimation of the wind velocity in the starting period, the model-predicted wave heights are smaller than those from the observed datasets (see Fig. 7). In the peak period of wave height, the model predictions are relatively consistent with the observations.

4 Effect of Radiation Stress on Storm Surges

After a series of verifications, the model can be applied

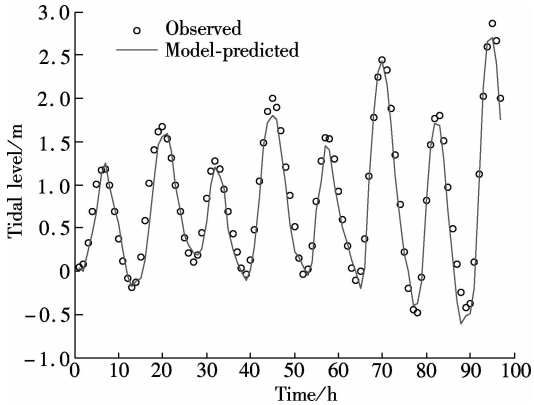

Fig. 6 Comparison between model-predicted and observed tidal levels at Hengsha station

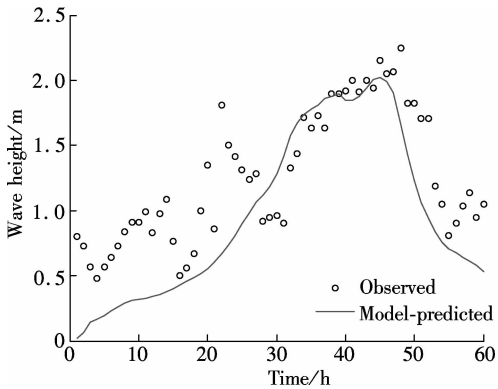

Fig. 7 Comparison between model-predicted and observed wave height at Xiangshui station

to simulate the storm surges and wave process on the coast of Jiangsu Province. Typhoon Muifa was generated around the northwestern Pacific Ocean. As Muifa moved northward, it created large waves that radiated outward and affected most of the East China Sea. As shown in Fig. 8, the storm surge varies widely from deep water to nearshore estuaries and floodplains. It is apparent that storm surges are quite significant in nearshore areas since the bathymetry becomes shallow. In deep water, storm surge is merely around 0.5 m, and the peak surge occurred on the coast of Jiangsu Province, in the regions where the bathymetry is shallow. In the Yangtze estuary, storm surges reach 0.9 to 1.1 m, and the maximum value is more than 1.3 m. The water level induced by typhoon storm surges around coastal areas may result in coastal flooding, thus causing significant loss of life and property.

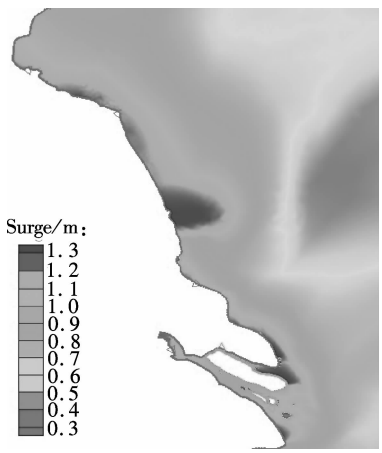

Fig. 8 The wave-induced storm surge in the coast of Jiangsu province

To analyze the effects of radiation stress on storm surges at different depths, a comparison is made between the wave-induced storm surge and storm surge without radiation stress. The radiation stress gradients are generated by the wave transformation drive set-up and currents. Wind-driven waves affect the vertical momentum mixing, which in turn affect the circulation. According to Fig. 9, there is no obvious difference between storm surges whether with radiation stress in deep water, because in deep water the wave cannot break. However, behind the breaking zones, the wave-induced storm surge accounts for 0.06 to 0.1 m throughout much of the region. These contributions are significant when they occur near the Yangtze estuary. The difference can reach 0.1 to 0.18 m. Although overall the effect of radiation stress is not very significant where the slope of this area is not very steep, the storm surge increased by radiation stress can reach 10 cm high/wide in the Yangtze estuary. For some regions with steep slope, the effects must be more remarkable. Thus, radiation stress cannot be ignored when simulating storm surges. It is worth mentioning that the bathymetry in some areas of the Jiangsu coast may not be as accurate as those in the Yangtze estuary. Thus, the simulation accuracy of storm surges and wave heights needs to be improved by introducing more accurate local bathymetry.

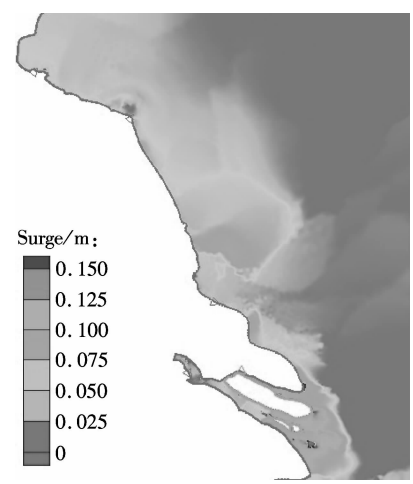

Fig. 9 Changes in storm surge levels (model with radiation stress minus the model without radiation stress)

5 Conclusion

This paper applies the ADCIRC + SWAN model in order to analyze storm surge behavior on the coast of Jiang-

su Province during Typhoon Muifa (1109). The highest surge during Typhoon Muifa occurred in the Yangtze estuary, where the value was up to 1.3 m. The storm surges along the coast of Jiangsu Province were about 1.1 m in contrast to the 0.5 m in deep water. The comparison analysis of the storm surge simulation with waves considered or does not show that radiation stress can increase water levels during the typhoon process. In deep water, the effects can be ignored, however, these become apparent when the wave moves into the breaking zones. The storm surge increased by radiation stress reaches 0.06 to 0.1 m throughout most of the studied regions in the Yangtze Estuary, and the increment may be up to 0.1 to 0.18 m.

The results provided in this paper show that the effects of radiation stress are significant when predicting the storm surge. Thus, in the coast of Jiangsu Province, especially, the Yangtze estuary, the waves and circulation processes should be coupled. The model-predicted storm surge along the coast of Jiangsu Province can be employed in coastal protection and flood mitigation.

References

[1] Kantha L. Classification of hurricanes: lessons from Katrina, Ike, Irene, Isaac and Sandy [J]. *Ocean Engineering*, 2013, **70**: 124 - 128.

[2] Knabb R D, Rhome J R, Brown D P. Tropical cyclone report: Hurricane Katrina, 23-30 August, 2005 [EB/OL]. (2005-12-20) [2014-08-17]. http://www.nhc.noaa.gov/pdf/TCR-AL122005_Katrina.pdf.

[3] Zhang Q, Wu L G, Liu Q F. Tropical cyclone damages in China 1983—2006 [J]. *Bulletin of the American Meteorological Society*, 2009, **90**(4): 489 - 495.

[4] von Storch H. Storm surges: phenomena, forecasting and scenarios of change [J]. *Procedia IUTAM*, 2014, **10**: 356 - 362.

[5] Sebastian A, Proft J, Dietrich J C, et al. Characterizing hurricane storm surge behavior in Galveston Bay using the SWAN + ADCIRC model [J]. *Coastal Engineering*, 2014, **88**: 171 - 181.

[6] Xu S D, Huang W R. Integrated hydrodynamic modeling and frequency analysis for predicting 1% storm surge [J]. *Journal of Coastal Research*, 2008 (52): 253 - 260.

[7] Funakoshi Y, Hagen S C, Bacopoulos P. Coupling of hydrodynamic and wave models: case study for Hurricane Floyd (1999) hindcast [J]. *Journal of Waterway, Port, Coastal, and Ocean Engineering*, 2008, **134**(6): 321 - 335.

[8] Dietrich J C, Zijlema M, Westerink J J, et al. Modeling hurricane waves and storm surge using integrally-coupled, scalable computations [J]. *Coastal Engineering*, 2011, **58**(1): 45 - 65.

[9] Xu S D, Huang W R, Zhang G P, et al. Integrating Monte Carlo and hydrodynamic models for estimating extreme water levels by storm surge in Colombo, Sri Lanka [J]. *Natural Hazards*, 2014, **71**(1): 703 - 721.

[10] Chang H. More than 3.6 million people suffered in Liaoning, Shanghai, Jiangsu, Zhejiang, Shandong during typhoon Muifa [EB/OL]. (2011-08-09) [2014-08-17]. http://news.weather.com.cn/1443798.shtml. (in Chinese)

[11] Luettich R A, Westerink J J. Formulation and numerical implementation of the 2D/3D ADCIRC finite element model version 44.XX [EB/OL]. (2004-08-12) [2014-08-17]. http://www.unc.edu/ims/adcirc/publications/2004/2004_Luettich.pdf.

[12] Huang W R, Xu S D. Neural network and harmonic analysis for recovering missing extreme water-level data during Hurricanes in Florida [J]. *Journal of Coastal Research*, 2009, **25**(2): 417 - 426.

基于波流耦合模型的江苏沿海风暴潮数值模拟

徐宿东[1] 殷 锴[1] 黄文锐[2,3] 郑 炜[1]

([1] 东南大学交通学院, 南京 210096)

([2] 同济大学土木工程学院, 上海 200092)

([3]Department of Civil and Environmental Engineering, Florida State University, Tallahassee, FL 32310, USA)

摘要:为了方便工程设计以及沿海防洪减灾,对可能由台风引起的风暴潮进行了研究.利用三角形非结构网格建立 ADCIRC 水动力模型和 SWAN 波浪模型的耦合模型,并将其应用于江苏沿海风暴潮和波浪研究.风速、潮位和波高的验证表明该 ADCIRC + SWAN 耦合模型可以很好地模拟研究区域的水位和波高.研究结果表明辐射应力对风暴潮计算结果有影响,且在如江苏沿海和长江口此类的浅水区域影响更为显著.模型计算的水位结果在江苏沿海得到工程应用,例如风暴潮预警和极端水位预测.

关键词:江苏沿海;台风风暴潮;ADCIRC 模型;SWAN 模型

中图分类号:U698.91